X-ray properties and interface study of B4C/Mo and B4C/Mo2C periodic multilayers

Fadi Choueikani, Françoise Bridou, B. Lagarde, Evgueni Meltchakov, François Polack, P. Mercere, Franck Delmotte

Appl Phys A
DOI 10.1007/s00339-013-7560-3

Applied Physics A
Materials Science & Processing

RAPID COMMUNICATION

X-ray properties and interface study of B_4C/Mo and B_4C/Mo_2C periodic multilayers

F. Choueikani · F. Bridou · B. Lagarde · E. Meltchakov · F. Polack · P. Mercere · F. Delmotte

Received: 9 January 2013 / Accepted: 10 January 2013

Abstract We present a comparative study of B_4C/Mo and B_4C/Mo_2C periodic multilayer structures deposited by magnetron sputtering. The characterization was performed by grazing incidence X-ray reflectometry at two different energies and high resolution transmission electron microscopy. The experimental results indicate the existence of an interdiffusion layer at the B_4C-on-Mo interface in the B_4C/Mo system. Thus, the B_4C/Mo multilayers were modeled by an asymmetric structure with three layers in each period. The thickness of B_4C-on-Mo interfacial layer was estimated about 1.1 nm. The B_4C/Mo_2C multilayers present less interdiffusion and are well modeled by a symmetric structure without interfacial layers. This study shows that B_4C/Mo_2C structure is an interesting alternative to B_4C/Mo multilayer for X-ray optic applications.

1 Introduction

Multilayer mirrors are widely used for different applications in extreme ultra-violet (EUV) (solar physics, photolithography) [1–4] and soft X-ray [5, 6]. Even if several two-component multilayer mirrors have been produced and studied such as B_4C/Mo [7], B_4C/Si [10], Ir/Si [11], Mo_2C/Si [4], the Mo/Si system remains the most studied for EUV applications. High quality mirrors made from this material pair have been demonstrated for 10–50 nm wavelength range (25–125 eV) [8, 9]. A key point that allowed the achievement of high reflectivity is the study and improvement of interface imperfections, such as layer roughness and interdiffusion. The composition and thickness of Mo/Si interfaces have been studied [12–15]. Several approaches were proposed to improve reflectivity taking into consideration these interfacial properties such as the sputtering a B_4C barrier layer between Mo and Si layers in order to prevent interdiffusion [14, 16–18]. Some authors have also proposed to replace the Mo by Mo_2C in order to increase thermal stability and/or to reduce the mechanical stress. Interesting results have been published concerning Mo_2C/Si [4] and Mo_2C/Be [19] systems. On the other hand, the Mo_2C is used as diffusion barrier for copper metallization [20] to prevent the copper diffusion in silicon for Cu/Si system. Concerning the B_4C/Mo multilayers, Barthelmess et al. have shown that the interfaces are not perfect and that the presence of interdiffusion layers limit the normal incidence reflectivity at 6.7 nm [7]. However, we found no study in the literature on the characterization of these interfacial layers.

In this paper, we focus on the B_4C/Mo and B_4C/Mo_2C systems for potential applications in the energy range 500–2500 eV (≈0.5–2.5 nm). In particular, there is a need for an efficient multilayer system with symmetrical interface properties to be used in the fabrication of Alternate Multi-Layer (AML) grating. Such AML gratings allow a high efficiency for first order of diffraction and a rejection of the other orders [5, 6]. Thus, we present in this paper a comparative study of interface properties of B_4C/Mo and B_4C/Mo_2C periodic multilayers. The main objectives of this study were

F. Choueikani (✉) · F. Bridou · E. Meltchakov · F. Delmotte
Laboratoire Charles Fabry, Institut d'Optique, CNRS, Univ Paris Sud, 2 avenue Augustin Fresnel, 91127 Palaiseau Cedex, France
e-mail: choueikani@synchrotron-soleil.fr

Present address:
F. Choueikani
Synchrotron SOLEIL, L'Orme des Merisiers, Saint-Aubin, BP48, 91192 Gif-sur-Yvette, France

B. Lagarde · F. Polack · P. Mercere
Synchrotron SOLEIL, L'Orme des Merisiers, Saint-Aubin, BP48, 91192 Gif-sur-Yvette, France

Published online: 18 January 2013

to characterize the thickness of each deposited layer at subnanometric scale, and to assess the existence of any interdiffusion layer between two consecutive layers in each system. It is organized as follow: at first, the experimental procedures to fabricate the multilayers and the characterization techniques are briefly presented. The main part deals with X-ray reflectivity measurements performed at grazing incidence at different wavelengths and the numerical adjustment with the modeling of the two systems. Then, a qualitative observation and analysis of high resolution transmission electron microscopy (HTEM) images are presented and discussed for both multilayer systems.

2 Experiments

2.1 Sample preparation

A magnetron sputtering deposition system, described elsewhere [21, 22], was used to fabricate B_4C/Mo and B_4C/Mo_2C multilayers. During the process, the chamber of preparation has a nominal vacuum of 5×10^{-8} Torr (mbar). The sputtering was performed with argon gas at a pressure of 2 mTorr. The targets size was 200 × 80 mm. The radio-frequency power was 150 W for B_4C target and a direct current of 0.06 A and 0.07 A was used for Mo and Mo_2C targets, respectively. In order to obtain a high homogeneity, the samples were rotated at 50 rpm, while passing over the targets with a velocity about 1°/s. The number and the velocity of scans determine the thickness of sputtered material. Multilayers with different expected thicknesses of B_4C, Mo and Mo_2C, were deposited on silicon polished substrates. The number of periods was fixed at 15 for all samples. The expected parameters for each sample are summarized in Tables 1 and 2. The deposition parameters that provide the expected thickness were deduced from calibrations on single-layer thin films.

2.2 Characterizations

Characterization of multilayers was performed with X-ray reflectivity measurements in grazing incidence. The experimental reflectivity curves were obtained using a goniometer BRUKER-DISCOVER D8 that works at the copper K-alpha radiation of 0.154 nm (≈8 keV). In the bench geometry, the sample stays at a fixed position. The reflectivity spectra versus grazing incidence angle were measured by moving the source arm, while tracking the reflected beam with the detector arm ($\theta - \theta$ scan configuration). The source arm consists of an X-ray tube, a collimating Gobel Mirrors providing high flux density, a rotary absorber, a 0.1 mm divergence slits and a Soller slits. The arm of detection consists of secondary Soller slits placed between two 0.1 mm divergence slits and a scintillator. The mechanical precision on angles is better than 0.01° and the angular resolution is about 0.01°.

Characterization of the multilayers was also performed on the soft X-ray branch of the Metrology and Tests Beamline at synchrotron SOLEIL [23]. For the experiment, a 1200 lines/mm VLS plane grating was used in order to cover an energy range between 400 and 1700 eV. Measurements were performed with constant exit slits opening, leading to a spectral resolution ranging from 4000 at the lower end to 500 at the higher end of the range. Flux at the sample position was about few 10^{10} photons/s in the $200 \times 100\ \mu m^2$ FWHM focal spot and the spectral purity was more than 99 %. The reflectivity spectra versus grazing incidence angle were measured by moving the sample, while tracking the reflected beam with the detector arm (θ–2θ scan configuration). Silicon AXUV-100 photodiode with aluminum flash coating was used to detect the reflected signal.

In a first stage, a homemade Fourier transform analysis of the reflectivity curve [24] was used in order to give a first approximation of the number of layers and of their thickness. By fitting the reflectivity curve using a trial and error method, the grazing X-ray reflectometry allows the determination of thickness, the interfacial roughness and the complex index ($n = 1 - \delta - i\beta$ where δ is the unit decrement of the refractive index and β is the extinction coefficient) of each of the successive films deposited on the substrate [25, 26].

Table 1 Expected parameters for B_4C/Mo multilayers. The number of periods is 15 for all samples

Sample	B_4C thickness (nm)	Mo thickness (nm)	Expected period (nm)
A1	0.63	2.50	3.13
A2	1.25	2.50	3.75
A3	2.50	2.50	5.00
A4	5.00	2.50	7.50
A5	2.50	1.24	3.74
A6	2.50	5.00	7.50
A7	2.50	74.5	9.95

Table 2 Expected parameters for B_4C/Mo_2C multilayers. The number of periods is 15 for all samples

Sample	B_4C thickness (nm)	Mo thickness (nm)	Expected period (nm)
B1	0.75	2.5	3.25
B2	1.31	2.5	3.81
B3	2.63	2.50	5.13
B4	5.26	2.50	7.76
B5	2.50	0.63	3.13
B6	2.50	1.25	3.75
B7	2.50	5.00	7.50
B8	2.50	2.50	5.00

A high resolution transmission electron microscopy (HRTEM) was used to study the structure of the as-deposited multilayers. The analyses were performed using the microscope FEI-TECNAI G2 F20 S-TWIN operating at 200 kV located at SERMA TECHNOLOGIES of Grenoble in France. Cross-sectional TEM specimens were prepared with the focused ion beam technic using FEI-FIB Strata DB400.

3 Results and discussion

3.1 B_4C/Mo multilayers

Two sets of B_4C/Mo multilayers are presented in Table 1. In the first set (samples A1 to A4), the expected thickness of Mo layers was fixed at 2.50 nm while the B_4C expected thickness varied between 0.63 and 5.00 nm. In the second set (sample A3 and A5 to A7), the expected thickness of B_4C was fixed at 2.5 nm and the expected thickness of Mo varied.

The period thickness, the thickness and the unit decrement of the refractive index δ of the individual layers, as well as the interface roughness of all multilayer systems have been determined by fitting X-ray reflectometry measurements. An example of X-ray reflectivity measurement under grazing incidence at 0.154 nm and the corresponding theoretical adjustment that was performed with a model of two layers in the period are illustrated in Fig. 1 for sample A4. Figure 1 shows that the fit with a model of two layers in the period is not in good agreement with the experimental curve. In particular, it was not possible to obtain a good fit of the intensity of Bragg's peaks with this simple model. This indicates that the model of two layers in the periods is not appropriate for the B_4C/Mo multilayers. The properties deduced from this fit are summarized in line A4* into Table 3. In comparison with the thickness of each layer, the roughness is remarkably high (4.32 nm) at the B_4C-on-Mo interface while it is relatively lower (1.40 nm) at the Mo-on-B_4C one. These asymmetric values of roughness suggest the presence of an interdiffusion layer at the B_4C-on-Mo interface. The same experimental curve (sample A4) and its corresponding numerical adjustment that was performed with a model of three layers in the period are illustrated in Fig. 2. This figure shows a very good agreement between the experimental measurement and the fit.

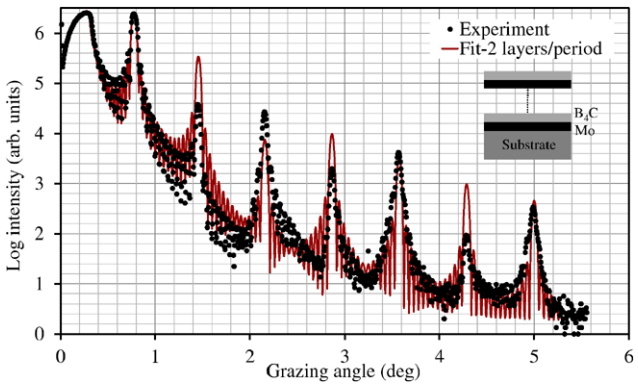

Fig. 1 Grazing incidence X-ray reflectivity of sample A4 measured (*dots*) at 0.154 nm and fitted one with a model of two layers in the period (*continuous*). The expected thickness of B_4C/Mo is 5.00 nm. The figure in *the inset* presents the model of two layers: B_4C/Mo

Therefore, the interlayer regions are asymmetric. The deposition of B_4C on Mo leads to the creation of an interfacial layer whereas the deposition of Mo on B_4C leads to a sharp interface (see the model in the inset of Fig. 2). It should be noted that the δ values for the B_4C and Mo layer are, respectively, around 0.7×10^{-5} and 2.7×10^{-5} which are slightly smaller than the theoretical values 0.75×10^{-5} and 2.86×10^{-5} [27]. The δ value of the interfacial layer is ranged between those of B_4C and Mo. It is around 1.9×10^{-5}. The properties of all samples of the two sets deduced from the model of three layers in the period are summarized in Table 3.

The evolution of the fitted thicknesses of B_4C (lozenge points), B_4C-on-Mo called IL (triangle points) and Mo (square points) layers as a function of the B_4C expected thickness for samples A1 to A4 is given in Fig. 3. The expected thickness of Mo is 2.5 nm. Table 4 shows that the

Table 3 Parameters of the B_4C/Mo multilayers deduced from the numerical adjustment using a model of three layers in the period. The A4* line corresponds to a fit with a model of two layers in the period

Sample	Thickness (nm)			Period (nm)	δ ($\times 10^{-5}$)			Roughness (nm)		
	B_4C	IL	Mo		B_4C	IL	Mo	B_4C	IL	Mo
A1	0.00	0.91	1.95	2.86	–	1.95	2.75	–	0.38	0.19
A2	0.00	1.33	1.87	3.20	–	1.97	2.70	–	0.37	0.20
A3	1.09	1.20	1.97	4.26	0.66	1.84	2.71	0.33	0.21	0.17
A4	3.08	1.04	2.09	6.21	0.68	1.87	2.72	0.28	0.20	0.17
A4*	4.17	–	2.03	6.20	0.82	–	2.90	1.40	–	4.32
A5	0.92	1.10	1.04	3.06	0.68	1.85	2.70	0.30	0.26	0.17
A6	1.01	1.26	4.46	6.73	0.67	1.84	2.73	0.32	0.22	0.17
A7	0.86	1.20	6.38	8.44	0.66	1.87	2.68	0.26	0.33	0.19

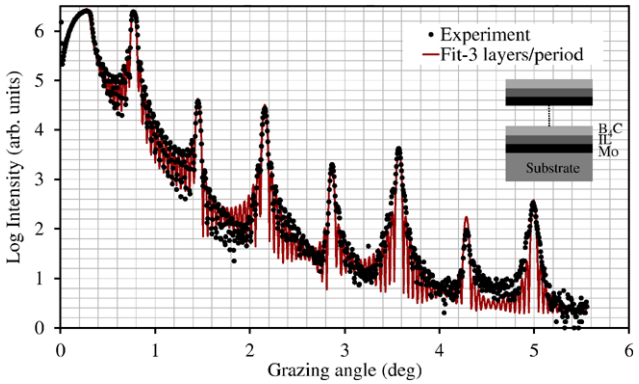

Fig. 2 Grazing incidence X-ray reflectivity of the sample A4 that was measured (*dots*) at 0.154 nm and fitted with a model of three layers in the period (*continuous*). The expected thickness of B_4C is 5.00 nm. The figure in *the inset* presents the model of three layers: B_4C/IL/Mo where IL is the B_4C-on-Mo interfacial layer

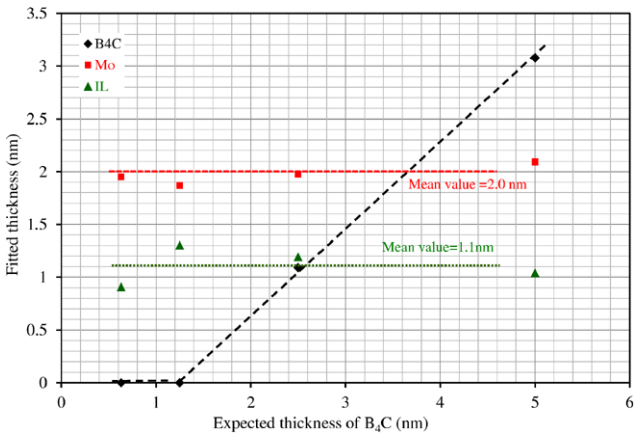

Fig. 3 Variation of B_4C, B_4C-on-Mo (IL) and Mo fitted thicknesses as functions of B_4C expected thickness. The expected Mo thickness is 2.5 nm for all samples. The *dashed lines* are guides for the eyes

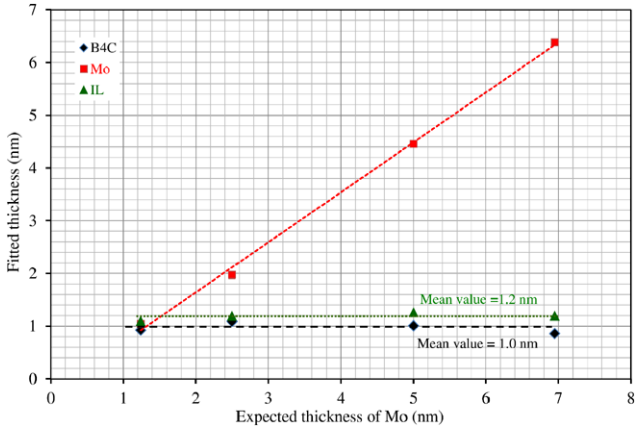

Fig. 4 Variation of B_4C, B_4C-on-Mo and Mo fitted thicknesses as functions of Mo expected thickness. The expected B_4C thickness is 2.50 nm for all samples

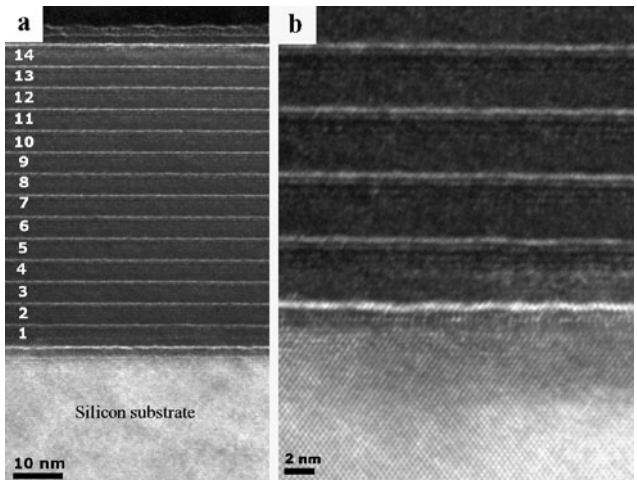

Fig. 5 Transmission electron microscopy cross-sectional images of the sample A3 (see Table 1). The scale bar is 10 nm for the micrograph A and 2 nm for the micrographs B

period deduced from the fit is always smaller than the expected one. The Mo thickness is reduced from 2.5 to 2 nm. The diminution of the B_4C thickness is around 1.5 nm. The thickness of the interfacial layer IL is around 1.1 nm. Therefore, each B_4C layer that has an expected thickness lower than 1.5 nm (A1 and A2 samples) completely vanishes to lead to the creation of an interfacial layer. Then, the system can be fitted with a model of two layers: IL/Mo. This result is confirmed with the other set of samples in which the expected thickness is fixed at 2.5 nm for B_4C and varies between 1.25 and 7.45 nm for Mo (see Table 1). We have plotted in Fig. 4 the variation of the fitted thicknesses of B_4C, IL and Mo with the expected thickness of Mo layers for this second set of samples.

This figure shows that the thickness of the B_4C layer is about 1 nm (reduction of 1.50 nm from its expected value) while the thickness of Mo is 0.50 nm smaller than the expected one. The thickness of the interfacial layer is around 1.10 nm.

High resolution Transmission electron microscopy (HTEM) micrographs of A3 sample (B_4C/Mo; see Table 1 for details) are shown on Fig. 5. The expected thickness of Mo and B_4C layers for this sample are 2.50 nm. The scale bar of image A is 10 nm while it is of 2 nm for image B. In fact, the molybdenum has a higher atomic number ($Z = 42$) and therefore appears darker as it scatters more electrons than boron carbide. The TEM micrograph A show the very good regularity of the deposition process in thickness and roughness through the coating. The micrograph B indicates that the Mo layers are amorphous. In addition, the period deduced from both images is 4.35 nm which is in good agreement with the value obtained by X-ray reflectometry. We can clearly see on both micrographs that the Mo-on-B_4C interface is well defined and sharp whereas the B_4C-

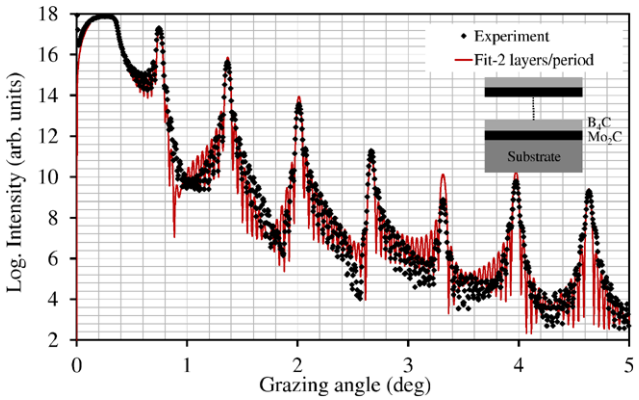

Fig. 6 Grazing incidence X-ray reflectivity at 0.154 nm measured (*dots*) and fitted with a model of two layers in the period (*continuous*). The graph correspond the sample B7 which is described in Table 2

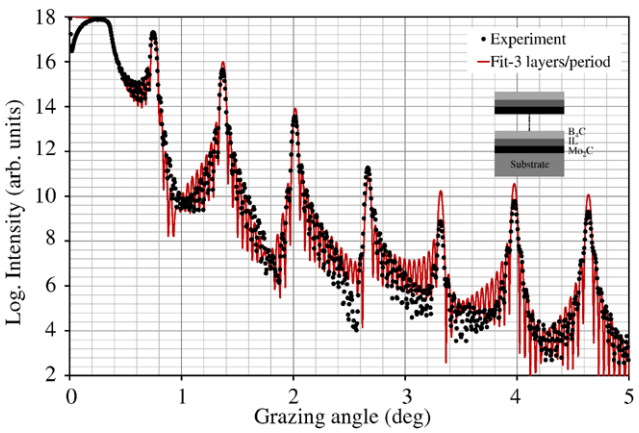

Fig. 7 Grazing incidence X-ray reflectivity at 0.154 nm measured (*dots*) and fitted with a model of three layers in the period (*continuous*). The graph corresponds to the sample B7* which is described in Table 2

on-Mo interface is more diffuse. In fact, it is difficult to distinguish, on image B, the IL and B_4C layers in each period in order to determine their exact thickness. The average thickness of the molybdenum layer per period is around 2.16 ± 0.09 nm which is close the value obtained by X-ray reflectometry. The total thickness of B_4C and IL layers is around 2.05 ± 0.09 nm. The more bright part corresponds to the B_4C material while the more contrasted one is for IL. Thus, the HTEM measurements on the B_4C/Mo systems confirm the result obtained from the optical characterization. The B_4C/Mo multilayers present a B_4C-on-Mo interfacial layer that can be approximated with an asymmetric model of three layers in the period.

3.2 B_4C/Mo_2C multilayers

The details of the two sets of B_4C/Mo_2C system deposited with the same sputtering parameters are described in Table 2. The first set consists of samples B1 to B4 with an expected Mo_2C thickness of 2.5 nm and with a varying thickness of B_4C (from 0.75 to 5.26 nm). In the second set (sample B5 to B8), the expected thickness of B_4C was fixed at 2.5 nm while that of Mo_2C varied from 0.63 to 5.00 nm.

Figure 6 (resp. Fig. 7) shows an example of grazing incidence X-ray reflectivity measurement at 0.154 nm and its corresponding numerical fit for a B_4C/Mo_2C multilayer using a model of two (resp. three) layers in the period. The parameters of these fits are given in the lines B7 (2 layers/period) and B7* (3 layers/period) of Table 4.

The comparison between Figs. 6 and 7 shows that both models of numerical adjustment can be appropriated for modeling of the B_4C/Mo_2C system. The addition of an interfacial layer in the model do not improve the fit. This means that, if an interfacial layer exists in the structure, it is thin enough and has no significant effect on the reflectivity spectra. These results were confirmed by measurements performed on Soft X-ray branch of Metrology and Tests

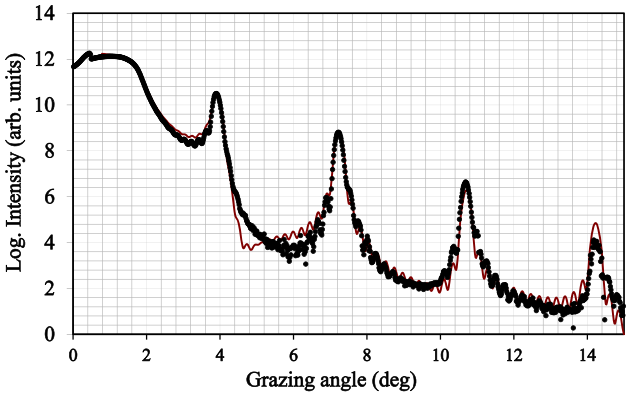

Fig. 8 Grazing incidence X-ray reflectivity at 0.83 nm measured for the sample B7 (*dots*) and fitted with a model of two layers in the period (*continuous*)

Beamline of Synchrotron SOLEIL. The experimental curve measured at 0.83 nm (1500 eV) on sample B7 with its corresponding numerical adjustment, is plotted on Fig. 8. The fitted thicknesses of Mo_2C and B_4C layers are, respectively, 5.1 nm and 1.6 nm. These values are in good agreement with those obtained at 0.154 nm. Thus, a simple model with two layers in the period, is sufficient to model the X-ray reflectivity performances of B_4C/Mo_2C multilayers.

The fitting results deduced from the numerical adjustments using a model of two layers in the period are summarized in Table 4 for the others B_4C/Mo_2C samples. The mean values of the decrement of the refractive index are, respectively, 2.47×10^{-5} and 0.72×10^{-5} for Mo_2C and B_4C layers. They are close to the theoretical values, which are 2.59×10^{-5} for Mo_2C and 0.75×10^{-5} for B_4C [27]. The evolution of the fitted thicknesses of B_4C and Mo_2C with the B_4C expected thickness is given in Fig. 9 for the first set of samples. These results show that the average value of fitted Mo_2C thicknesses (squares) is slightly higher

Table 4 Properties of the B_4C/Mo_2C multilayers deduced from fits using a model of two layers in the period. The thickness is in nm. B7* line corresponds to the fit using a model of three in the period

Sample	Thickness (nm)			Period (nm)	δ ($\times 10^{-5}$)			Roughness (nm)		
	B_4C	IL	Mo_2C		B_4C	IL	Mo_2C	B_4C	IL	Mo_2C
B1	0.09	0.00	2.59	2.68	0.80	–	2.36	0.27	–	0.36
B2	0.76	0.00	2.55	3.31	0.72	–	2.50	0.19	–	0.41
B3	1.87	0.00	2.68	4.55	0.67	–	2.58	0.19	–	0.34
B4	4.19	0.00	2.76	6.95	0.72	–	2.54	0.15	–	0.32
B5	1.95	0.00	1.08	3.03	0.72	–	2.45	0.17	–	0.36
B6	1.90	0.00	1.55	3.45	0.72	–	2.39	0.18	–	0.20
B7	1.48	0.00	5.21	6.69	0.72	–	2.48	0.15	–	0.30
B7*	1.44	0.50	4.75	6.69	0.70	1.53	2.55	0.15	0.17	0.30
B8	1.78	0.00	2.65	4.43	0.68	–	2.56	0.19	–	0.32

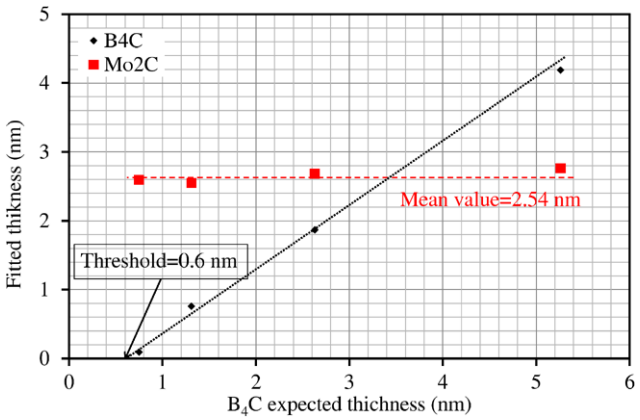

Fig. 9 Variation of B_4C and Mo_2C fitted thicknesses with B_4C expected thickness. The expected Mo_2C thickness is 2.5 nm for all samples. The *dashed lines* are the linear regression

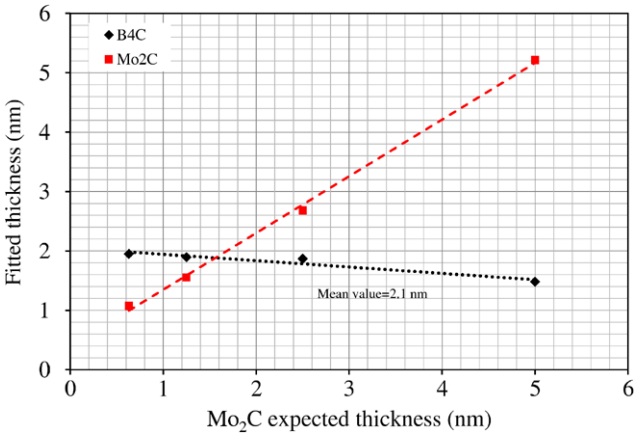

Fig. 10 Variation of B_4C and Mo_2C fitted thicknesses with Mo_2C expected thickness. The expected B_4C thickness is 2.5 nm for all samples. The *dashed lines* are linear regressions

(≈2.54 nm) than the expected one (2.5 nm). The graph (Fig. 9) presents also a linear variation of the fitted thickness of B_4C (lozenges) as a function of the expected ones. In comparison with the expected values, the fitted values of B_4C thickness are lower. The difference between expected and fitted thicknesses increases when the expected thickness increases. For example, the reduction value is around 0.66 nm for an expected thickness of 0.75 nm while it is around 1.07 nm for an expected thickness of 5.26 nm. Moreover, extrapolation of this linear variation suggests that, for an expected thickness lower than 0.6 nm, the final thickness of B_4C will vanish.

The variation of the fitted thickness of B_4C (lozenges) and Mo_2C (squares) layers as function of the expected thickness of Mo_2C is presented in Fig. 10 for the second set of samples.

This graph confirms the behavior that is observed in Fig. 9. In fact, it shows also that the thickness of B_4C layers decreases when the Mo_2C thickness increases. In order to obtain more details of the structure of the B_4C/Mo_2C multilayers, HTEM measurements were performed on an additional sample (B8, see Table 4) and results are shown

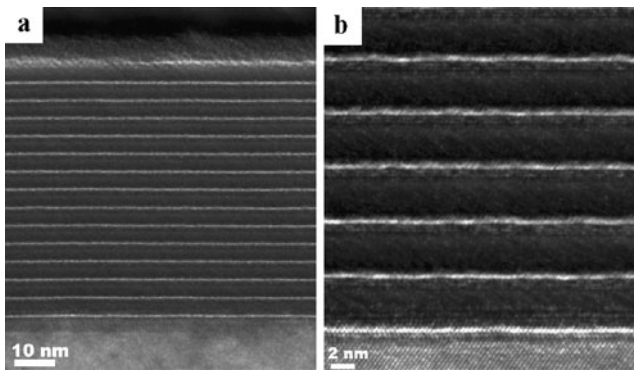

Fig. 11 Transmission electron microscopy cross-sectional images of a B_4C/Mo_2C sample (B8) in which the expected thickness of each layer is 2.5 nm. The scale bar is 10 nm for the micrograph A and 5 nm for the micrographs B

on Fig. 11. The expected thickness of each layer in the period is 2.5 nm. The image A shows that the period is 4.38 ± 0.03 nm. This value is in good agreement with results obtained by X-ray reflectometry measurements (see

Table 5 Reflectivity values of samples that were measured at 1500 eV using the soft X-ray branch of Metrology and Tests Beamline

Sample	A3	A6	B3	B7
Expected thickness (nm)				
B_4C/Mo or Mo_2C	25/25	25/50	26.5/25	25/50
Reflectivity (%)	13.2	13.7	16.5	15.7

Table 4). It shows an average thickness for the Mo_2C layer around 2.4 ± 0.04 nm while the thickness of the B_4C layer is 1.93 ± 0.04 nm. The image B looks similar to the case of B_4C/Mo multilayer (Fig. 5) with a sharp Mo_2C-on-B_4C interface and a more diffused Mo_2C-on-B_4C interface.

Finally, the reflectivity of the first Bragg peak was measured at 1500 eV for samples A3, A6, B3 and B7. The results are summarized into Table 5 For a same expected thickness, the B_4C/Mo_2C systems (B3 and B7) present a reflectivity higher than the B_4C/Mo systems (A3 and A6).

4 Discussion

The results show the existence of asymmetric interfaces in B_4C/Mo multilayers that can be modeled by adding an interfacial layer in the system at the B_4C-on-Mo interface. This interfacial layer is about 1.1 nm thick and probably consists of a mixture of Mo_xB_y or Mo_xC_y materials. The characterization techniques (Grazing X-ray reflectivity and HTEM) do not allow determining the exact chemical composition of this interfacial layer. However, the existence of this B_4C-on-Mo interdiffusion layer is in good agreement with several published works [28–30]. Rooij-Lohmann et al. have used thin B_4C layers (typically less than 1 nm thick) as barrier layer between the silicon and molybdenum layers in Si/Mo multilayers, in order to improve the reflectivity. Their study highlights the role of the B_4C barrier as retarding agent of diffusion [28]. However, our results indicate that for a deposition thickness lower than around 1.25 nm, the B_4C layer has completely vanished. Thus, the true nature of the barrier layer is not B_4C but a mixture of B_4C and Mo (which we called here interdiffusion layer). We found no previous quantitative study in the literature related to the interdiffusion between B_4C and Mo layers. The existence of such an interfacial layer is a major drawback of this multilayer system for applications where index profile symmetry is required. This is the case in particular for the achievement of Multilayer Grating that allows a high efficiency in the range of 500–2500 eV [5, 6]. In this context, we propose to use an alternative system in which Mo layer is replaced by Mo_2C. The B_4C/Mo_2C system looks very similar to B_4C/Mo one on HTEM pictures. However, the Mo_2C-on-B_4C interface is less diffuse and X-ray reflectivity measurements show that this structure can be modeled with only two layers per period (no interfacial layer). The Mo_2C-on-B_4C interfacial layer, if it exists, is less that 0.5 nm thick and is below the sensitivity of grazing angle X-ray reflectometry. The theoretical density of Mo_2C, $\rho = 9.18$ g/cm^3, slightly lower than the density of Mo ($\rho = 10.2$ g/cm^3), provides a good density contrast with B_4C ($\rho = 2.25$ g/cm^3). Measurements with synchrotron radiation source at 1500 eV show that the Mo_2C/B_4C multilayers present higher reflectivity than the Mo/B_4C ones with similar structures. Thus, the Mo_2C/B_4C multilayer system provides high reflectivity and good symmetry of the optical index profile as shown by the model with two layers in the period. In addition, our results suggest that Mo_2C or a combination of B_4C and Mo_2C could be a better solution as barrier layers in Si/Mo or other Mo-based multilayers.

5 Conclusion

In this paper, we report on an experimental comparison between B_4C/Mo and B_4C/Mo_2C multilayer systems deposited by magnetron sputtering. The B_4C/Mo system has an interfacial layer, which thickness is approximately 1.1 nm, at the B_4C-on-Mo interface. Its X-ray performances were well simulated by using an asymmetric model with three layers in the period. The HTEM images confirm that asymmetry of this multilayer system with a sharp Mo-on-B_4C interface and a more diffuse B_4C-on-Mo interface. The B_4C/Mo_2C multilayers present a better symmetry of the optical index profile. We have shown that X-ray reflectivity can be well simulated with a model of two layers in the period, without interfacial layer. Moreover, the experimental reflectivity peak at 1500 eV is higher for B_4C/Mo_2C samples than for B_4C/Mo ones. Due to its symmetry, the B_4C/Mo_2C system is a promising solution for applications such as alternate multilayer gratings with a high efficiency.

Acknowledgements This work is supported by a grant from the RTRA (réseaux thématiques de recherche avancée) program "Triangle de la Physique". The deposition and the characterization of the multilayers were performed on CEMOX (Centrale d'Elaboration et de Métrologie d'Optique X), a platform of LUMAT federation (CNRS FR2764). The authors would like to thank Karine Rousseau from SERMA TECHNOLOGIES for performing HTEM investigation.

References

1. E. Meltchakov, C. Hecquet, M. Roulliay, S. De Rossi, Y. Menesguen, A. Jerome, F. Bridou, F. Varnière, M.-F. Ravet-Krill, F. Delmotte, Development of Al-based multilayer optics for EUV. Appl. Phys. A **98**, 111–117 (2010)
2. Y. Ménesguen, S. De Rossi, E. Meltchakov, F. Delmotte, Aperiodic multilayer mirrors for efficient broadband reflection in the extreme ultraviolet. Appl. Phys. A **98**, 305–309 (2010)
3. M. Suman, M. Pelizzo, P. Nicolosi, D.L. Windt, Aperiodic multilayers with enhanced reflectivity for extreme ultraviolet lithography. Appl. Opt. **47**, 2906–2914 (2008)

4. D.L. Windt, S. Donguy, J. Seely, D. Kjornrattanawanich, Experimental comparison of extreme-ultraviolet multilayers for solar physics. Appl. Opt. **43**, 1835–1848 (2004)
5. F. Polack, M. Idir, E. Jourdain, A. Liard-Cloup, Two-dimensional diffraction network with alternating multilayer stacks and method for the production thereof and spectroscopic devices comprising said networks. European Patent Application EP1700141 (2005)
6. F. Polack, B. Lagarde, M. Idir, A. Liard-Cloup, E. Jourdain, M. Roulliay, Alternate multilayer gratings with enhanced diffraction efficiency in the 500–5000 eV energy domain, in *Ninth International Conference on Synchrotron Radiation Instrumentation Daegu*. AIP Conf. Proceedings Series, vol. 879 (2007), pp. 489–492
7. M. Barthelmess, S. Bajt, Thermal and stress studies of normal incidence Mo/B_4C multilayers for a 6.7 nm wavelength. Appl. Opt. **50**, 1610–1619 (2011)
8. R.S. Rosen, D.G. Stearns, M.A. Viliardos, M.E. Kassner, S.P. Venon, Y. Cheng, Silicide layer growth rates in Mo/Si multilayers. Appl. Opt. **32**, 6975–6980 (1993)
9. S. Braun, H. Mai, M. Moss, R. Scholz, A. Leson, Mo/Si multilayers with different barrier layers for applications as extreme ultraviolet mirrors. Jpn. J. Appl. Phys. **41**, 4074–4081 (2002)
10. J.M. Slaughter, B.S. Medower, R.N. Watts, C. Tarrio, T.B. Lucatorto, C.M. Falco, Si/B4C narrow-bandpass mirrors for extreme ultraviolet. Opt. Lett. **19**, 1786–1788 (1994)
11. P. Zuppella, G. Monaco, A.J. Corso, P. Nicolosi, D.L. Windt, V. Bello, G. Mattei, M.G. Pelizzo, Iridium/silicon multilayers for extreme ultraviolet applications in the 20–35 nm wavelength range. Opt. Lett. **36**, 1203–1205 (2011)
12. D.L. Windt, R. Hull, W.K. Waskiewics, Imperfections in metal/Si multilayers. J. Appl. Phys. **71**, 2675–2678 (1992)
13. A. Patteli, J. Ravagnana, V. Rigatoa, G. Salmasoa, D. Silvestrinia, E. Bontempic, L.E. Deperoc, Structure and interface properties of Mo/B_4C/Si multilayers deposited by rf-magnetron sputtering. Appl. Surf. Sci. **238**, 262–268 (2004)
14. H. Maury, J.-M. André, J. Gautier, F. Bridou, F. Delmotte, M.-F. Ravet-Krill, P. Holliger, P. Jonnard, Physico-chemical study of the interfaces of Mo/Si multilayer interferential mirrors: correlation with the optical properties. Surf. Interface Anal. **38**, 744–747 (2006)
15. H. Maury, P. Jonnard, J.-M. André, J. Gautier, M. Roulliay, F. Bridou, F. Delmotte, M.-F. Ravet-Krill, A. Jérome, P. Holliger, Non-destructive X-ray study of the interphases in Mo/Si and Mo/B_4C/Si/B_4C multilayers. Thin Solid Films **514**, 278–286 (2006)
16. S. Bajt, J.B. Alameda, T.W. Barbee, W.M. Clift, J.A. Folta, B. Kaufmann, E.A. Spiller, Improved reflectance and stability of Mo–Si multilayers. Opt. Eng. **41**, 1797–1804 (2002)
17. T. Bottger, D.C. Meyer, P. Paufler, S. Braun, M. Moss, H. Mai, E. Beyer, Thermal stability of Mo/Si multilayers with boron carbide interlayers. Thin Solid Films **444**, 165–173 (2003)
18. I. Nedelcu, R.W.E. Van de Kruijs, A.E. Yakshin, F. Bijkerk, Microstructure of Mo/Si multilayers with B_4C diffusion barrier layers. Appl. Opt. **48**, 155–160 (2009)
19. S. Bajt, T.W. Barbee, High reflectance and low stress Mo_2C/Be multilayers. US Patent Application US 6,229,652 B1 (2001)
20. C.C. Tripathi, M. Kumar, D. Kumar, Atom beam sputtered Mo_2C films as a diffusion barrier for copper metallization. Appl. Surf. Sci. **255**, 3518–3522 (2009)
21. J. Gautier, F. Delmotte, M. Roulliay, F. Bridou, M.-F. Ravet, A. Jerome, Study of normal incidence of three-component maltilayer mirrors in the range 20–40 nm. Appl. Opt. **44**, 384–390 (2005)
22. J. Gautier, F. Delmotte, F. Bridou, M.-F. Ravet, F. Varniere, M. Rouilliay, A. Jerome, I. Vickridge, Characterization and optimization of magnetron sputtered Sc/Si multilayers for extreme ultraviolet optics. Appl. Phys. A **88**, 719–725 (2007)
23. M. Idir, P. Mercere, T. Moreno, A. Delmotte, P. Da Silva, M.H. Modi, Metrology and tests beamline at SOLEIL design and first results, in *Tenth. International Conference on Radiation Instrumentation Melbourne*. AIP Conf. Proceedings Series, vol. 1234 (2009), pp. 485–488
24. F. Bridou, B. Pardo, Grazing X-ray reflectometry data processing by Fourier transform. J. X-Ray Sci. Technol. **4**, 200–216 (1994)
25. L. Nevot, B. Pardo, J. Corno, Characterization of X-UV multilayers by grazing incidence X-ray reflectometry. Rev. Phys. Appl. **23**, 1675–1686 (1988)
26. F. Bridou, B. Pardo, Automatic characterisation of layers stacks from reflectivity measurements. Application to the study of the validity conditions of the grazing X-rays reflectometry. J. Opt. **21**, 183–191 (1990)
27. http://henke.lbl.gov/optical_constants/getdb2.html
28. V.I.T.A. de Rooij-Lohmann, A.W. Kleyn, F. Bijkerk, H.H. Brongersma, A.E. Yakshin, Diffusion and interaction studied nondestructively and in real-time with depth-resolved low energy ion spectroscopy. Appl. Phys. Lett. **94**, 063107 (2009)
29. V.I.T.A. de Rooij-Lohmann, L.W. Veldhuizen, E. Zoethout, A.E. Yakshin, R.W.E. van de Kruijs, B.J. Thijsee, M. Gorgoi, F. Schafers, F. Bijkerk, Enhanced diffusion upon amorphous-to-nanocrystalline phase transition in Mo/B_4C/Si layered systems. J. Appl. Phys. **108**, 014314 (2010)
30. V.I.T.A. de Rooij-Lohmann, L.W. Veldhuizen, E. Zoethout, A.E. Yakshin, R.W.E. van de Kruijs, B.J. Thijsse, M. Gorgoi, F. Schafers, F. Bijkerk, Chemical interaction of B_4C, B, and C with Mo/Si layered structures. J. Appl. Phys. **108**, 094314 (2010)